

Theoretical and Experimental Analysis of Stability Limits of Non-axisymmetric Liquid Bridges under Microgravity Conditions

In this paper the stability of non-axisymmetric liquid bridges under microgravity conditions is investigated. The influence on the stability of an almost cylindrical liquid bridge of axisymmetric effects like its volume, a small axial acceleration acting on it and unequal-diameter supporting disks, as well as that of non-axisymmetric perturbations like small lateral acceleration and non-coaxial supporting disks, has been analyzed by using standard bifurcation techniques. The expression for the maximum length of a liquid bridge, including all the above mentioned effects, has been obtained. In addition, the effect on the stability of liquid bridges having non-coaxial supporting disks has been experimentally studied within the constraints of an Earth laboratory by using millimetric liquid bridges. Analytical and experimental results show that each one of the non-axisymmetric perturbations like the ones here considered (lateral acceleration and eccentricity) can be, from the point of view of stability, as critical as axisymmetric perturbations. In addition, it is demonstrated that when both non-axisymmetric perturbations are not negligible, the coupling of both perturbations can be a stabilizing effect on the liquid bridge.

1 Introduction

The fluid configuration considered in this paper consists of an isothermal mass of liquid of volume V held by surface tension forces between two parallel solid disks (of radii \bar{R}_1 and \bar{R}_2 , respectively) placed a distance L apart. Both disks can be non-coaxial, $2\bar{E}$ being the distance between the disk axes (fig. 1). Such fluid configuration can be uniquely defined by the following dimensionless parameters: the dimensionless volume $V = V/(\pi\bar{R}_0^2L)$, where $\bar{R}_0 = (\bar{R}_1 + \bar{R}_2)/2$,

the slenderness $A = L/(2\bar{R}_0)$, the dimensionless eccentricity $e = \bar{E}/\bar{R}_0$, the dimensionless disk radii difference, $h = (\bar{R}_2 - \bar{R}_1)/(\bar{R}_2 + \bar{R}_1)$, the Bond number $B = \bar{\rho}\bar{g}\bar{R}_0^2/\bar{\sigma}$ (where $\bar{\rho}$ is the difference in densities between the liquid bridge and the surrounding medium, \bar{g} the acceleration acting on the liquid bridge and $\bar{\sigma}$ stands for the surface tension), the angle α between the direction on which Bond number acts and the liquid bridge axis, defined in fig. 1, and the angle β between the plane defined by the axes of the disks and the lateral component of the gravity acceleration.

As it is well-known, liquid bridges can lose their stability with respect to either axisymmetric or non-axisymmetric perturbations [1, 2]. However, in most of the papers dealing with liquid bridges, either from the theoretical or the experimental point of view, only axisymmetric configurations have been considered [3]. Concerning non-axisymmetric perturbations, some effort has been devoted to a non-axisymmetric instability which appears when the liquid bridge is rotated as a solid body. The pioneering experimental work was done on board *SkyLab 4* where a demonstration of the so-called C-mode was performed [4] with a not fully controlled excitation. The theoretical background for this instability can be found in [5, 6]. An experiment under well-controlled excitation was performed later on board a TEXUS sounding rocket, where the liquid bridge was rotated around an axis slightly shifted from that of the disks, the results being in good agreement with the theory [7].

The influence of a non-axisymmetric stimulus like a non-axial acceleration was analyzed by *Coriell, Hardy and Cordes* [8] for the case of cylindrical volume liquid bridges ($V=1$) with slendernesses close to the Rayleigh stability limit $A = \pi$. The same problem, but including the effect of the eccentricity of the supporting disks, was theoretically analyzed by *Perales* [9] although there was a mistake in one of his conclusions. Apart from these two last quoted papers, as far as we know, no more works dealing with static non-axisymmetric perturbations have been published, the knowledge on the behaviour of liquid bridges under non-axisymmetric perturbations being much smaller than the existing background on the behaviour of axisymmetric liquid bridges.

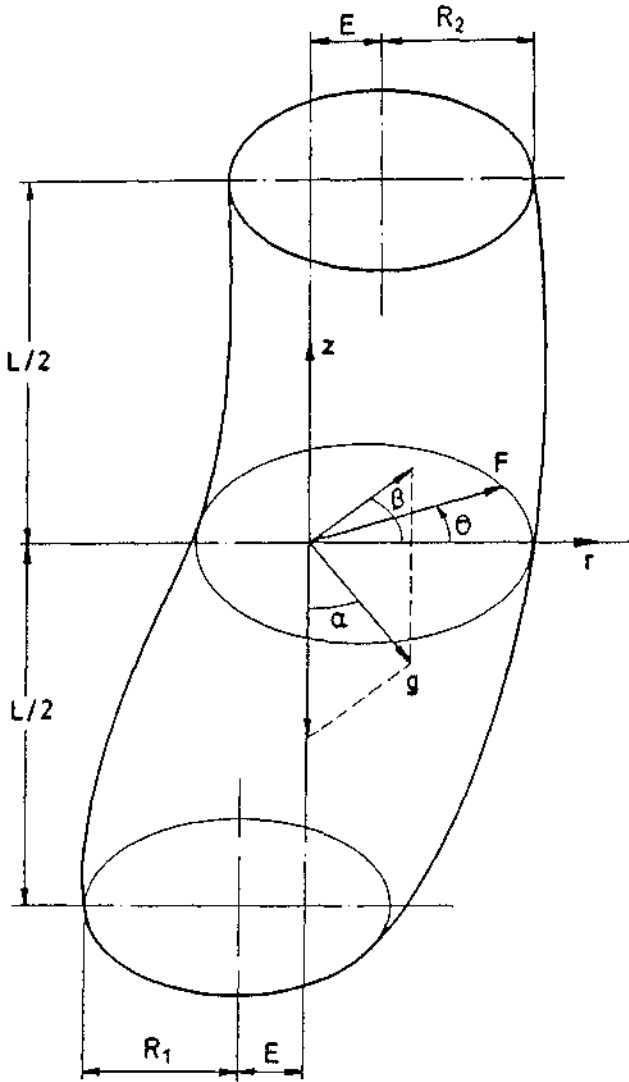


Fig. 1. Geometry and coordinate system for the liquid bridge problem

This paper is devoted to the analysis of the stability limits of liquid bridges under microgravity conditions with volume close to the cylindrical one ($V = 1$), slenderness close to π , and subjected to both axisymmetric and non-axisymmetric perturbations. The main conclusion that can be derived from the analytical results here presented is that the combined effect of both lateral acceleration and eccentricity can stabilize liquid bridges subjected to axial accelerations. Aiming to check the theoretical predictions, several experiments have been performed on Earth by using millimetric liquid bridges. In order to keep the experimental effort between reasonable limits, the study has been restricted to the analysis of the influence on minimum volume stability limits of the eccentricity of the disks of liquid bridges between equal disks ($h = 0$) subjected to either axial or lateral accelerations, the agreement between experimental results and theoretical predictions being good enough.

2 Mathematical Model

Equilibrium shapes of liquid bridges are described by the Young-Laplace equation, which in dimensionless variables reads

$$M(F) + P - B_a z + B_l F \cos(\theta - \beta) = 0, \quad (1)$$

where $M(F)$ is twice the mean curvature of the interface

$$M(F) = \{F[1 + (F_z)^2][F_{\theta\theta} - F] + FF_{zz}\{F^2 + (F_\theta)^2\} - 2F_\theta[F_\theta + FF_z F_{z\theta}]\} \cdot \{F^2[1 + (F_z)^2] + (F_\theta)^2\}^{-3/2}. \quad (2)$$

Boundary conditions are

$$F(\pm A, \theta) = [(1 \pm h)^2 - e^2 \sin^2(\theta)]^{1/2} \pm e \cos(\theta), \quad (3)$$

$$F(z, \theta + 2\pi) = F(z, \theta), \quad (4)$$

$$\frac{1}{2} \int_{-A}^A dz \int_0^{2\pi} F^2 d\theta = 2\pi AV. \quad (5)$$

To write down the above expressions all lengths have been made dimensionless with \bar{R}_0 ; B_a and B_l are the two components of Bond number, $B_a = B \cos(\alpha)$ and $B_l = B \sin(\alpha)$, respectively, and P is a constant related with the difference between the outer pressure, assumed constant, and the inner pressure, which has been made dimensionless with $\bar{\sigma}/\bar{R}_0$. The subscripts z and θ indicate derivatives with respect to z and θ , respectively.

Critical points result after linearization of the above formulation [9]. It is well-known that in the case $B_a = B_l = h = e = 0$, $V = 1$, the problem under consideration has the trivial equilibrium solution $F = 1$, $P = 1$ for any A . The introduction of the following expansions $F(z, \theta) = 1 + \epsilon f(z, \theta) + O(\epsilon^2)$, $P = 1 + \epsilon p + O(\epsilon^2)$, where ϵ stands for the magnitude of the deformation of the interface, allows us to calculate $f(z, \theta)$ after neglecting $O(\epsilon^2)$ terms in the problem formulation. All the solutions of the linear problem are axisymmetric, the expression for the interface deformation being non-trivial only for a discrete number of values of A ; the smallest value of A for which the bifurcation to non-cylindrical equilibrium shapes takes place is $A = \pi$, where the transition from stable to unstable equilibrium shapes occurs (all other bifurcation points are not relevant as they cannot be reached because the liquid bridge will break before). Therefore, the instability appears at $A = \pi$ and, within this approximation, the unstable equilibrium shapes are defined by $f(z, \theta) = \sin(\pi z/A)$, $p = 0$, which is the solution that must be perturbed to calculate the variation of the maximum stable slenderness for small values of the considered parameters.

From now on the process to obtain the variation of the maximum stable slenderness due to the different effects under consideration is similar to that described by Perales [9], although in that paper only non-axisymmetric effects ($B_a = h = 0$, $B_l \neq 0$, $e \neq 0$) and cylindrical volume liquid bridges ($V = 1$) were considered. First of all, a new variable, $x = \pi z/A$, which normalizes boundary conditions, $\lambda = 1 - A/\pi$, is introduced, and higher order terms than those appearing in the linear problem are retained. Let

$g(x, \theta)$ and q be the expressions representing these higher order terms in the expressions of the interface shape and the pressure, respectively. The new expansions for F and P are then $F(z, \theta) = 1 + \varepsilon \sin(x) + g(x, \theta)$, $P = 1 + q$, which, after substitution in eqs. (1)–(5), gives the new formulation:

$$\begin{aligned} M^*(1 + \varepsilon \sin(x) + g(x, \theta)) + 1 + q \\ + (1 + \varepsilon \sin(x) + g(x, \theta))B_l \cos(\theta - \beta) \\ - B_u x(1 - \lambda) = 0, \end{aligned} \quad (6)$$

$$g(\pm \pi, \theta) = \pm h \pm e \cos(\theta) - \frac{1}{2} e^2 \sin^2(\theta) + \dots, \quad (7)$$

$$g(x, \theta) = g(x, \theta + 2\pi), \quad (8)$$

$$\int_{-\pi}^{\pi} dx \int_0^{2\pi} [2g(1 + \varepsilon \sin(x)) + g^2] d\theta = 4\pi^2 \left[v - \frac{1}{2} \varepsilon^2 \right], \quad (9)$$

where, instead of V , a new parameter measuring the difference in volume with respect to that of a cylindrical liquid bridge, $v = V - 1$, has been used. Note that the curvature of the interface, M^* , is now computed in terms of the variables x and θ , so that M^* includes λ as a parameter. It must be pointed out that this formulation requires an additional condition in order to uniquely define the parameter ε , this condition being

$$\int_{-\pi}^{\pi} dx \int_0^{2\pi} g \sin(x) d\theta = 0. \quad (10)$$

The problem (6)–(10) allows us to calculate q and $g(x, \theta)$ in terms of λ, v, h, B_u, B_l , and e . As these parameters are assumed to be small enough, calculations can be performed by using standard perturbation techniques. It is known that this procedure requires the anticipation of certain properties of the solution, situation which can be avoided by using the idea of the bifurcation equation [10]. In this case, instead of eq. (6) the equation to be solved is

$$\begin{aligned} M^*(1 + \varepsilon \sin(x) + g(x, \theta)) + 1 + q \\ + (1 + \varepsilon \sin(x) + g(x, \theta))B_l \cos(\theta - \beta) \\ - B_u x(1 - \lambda) + \varphi \sin(x) = 0 \end{aligned} \quad (11)$$

and by using the Implicit Function Theorem [11] it is demonstrated that eqs. (7)–(11) uniquely define

$$\begin{aligned} g(x, \theta; \varepsilon, \lambda, v, h, B_u, B_l, e) \\ = \sum_{i=2}^7 \delta_i g_i(x, \theta) + \sum_{i=1}^7 \sum_{j=1}^7 \delta_i \delta_j g_{ij}(x, \theta) \\ + \sum_{i=1}^7 \sum_{j=1}^7 \sum_{k=1}^7 \delta_i \delta_j \delta_k g_{ijk}(x, \theta) + \dots, \end{aligned}$$

$$\begin{aligned} q(\varepsilon, \lambda, v, h, B_u, B_l, e) \\ = \sum_{i=2}^7 \delta_i q_i + \sum_{i=1}^7 \sum_{j=1}^7 \delta_i \delta_j q_{ij} + \sum_{i=1}^7 \sum_{j=1}^7 \sum_{k=1}^7 \delta_i \delta_j \delta_k q_{ijk} + \dots, \end{aligned}$$

$$\begin{aligned} \varphi(\varepsilon, \lambda, v, h, B_u, B_l, e) \\ = \sum_{i=2}^7 \delta_i \varphi_i + \sum_{i=1}^7 \sum_{j=1}^7 \delta_i \delta_j \varphi_{ij} + \sum_{i=1}^7 \sum_{j=1}^7 \sum_{k=1}^7 \delta_i \delta_j \delta_k \varphi_{ijk} + \dots, \end{aligned}$$

at least in a neighbourhood of $\varepsilon = \lambda = v = h = B_u = B_l = e = 0$ (in these last expressions $\delta_1 = \varepsilon, \delta_2 = \lambda, \delta_3 = v, \delta_4 = h, \delta_5 = B_u, \delta_6 = B_l, \delta_7 = e$). Such solutions will correspond to the solution of original set of eqs. (6)–(10) if and only if the parameters involved satisfy $\varphi(\varepsilon, \lambda, v, h, B_u, B_l, e) = 0$, which is called the bifurcation equation.

Before solving the problem it is convenient to analyze the symmetries involved in the problem which will allow us to anticipate some characteristics of the solution and to ease the algebra involved. As it can be seen through the inspection of the formulation, the problem is invariant under the following sets of symmetries:

$$\begin{aligned} x \rightarrow -x; \varepsilon \rightarrow -\varepsilon, h \rightarrow -h, B_u \rightarrow -B_u, e \rightarrow -e, \\ \varphi \rightarrow -\varphi \end{aligned} \quad (12)$$

$$\begin{aligned} x \rightarrow -x, \theta \rightarrow \theta + \pi; \varepsilon \rightarrow -\varepsilon, h \rightarrow -h, B_u \rightarrow -B_u, \\ B_l \rightarrow -B_l, \varphi \rightarrow -\varphi \end{aligned} \quad (13)$$

$$\theta \rightarrow \theta + \pi; B_l \rightarrow -B_l, e \rightarrow -e \quad (14)$$

and from these symmetries it is deduced that

$$\varphi(\varepsilon, \lambda, v, h, B_u, B_l, e) = -\varphi(-\varepsilon, \lambda, v, -h, -B_u, B_l, -e), \quad (15)$$

$$\varphi(\varepsilon, \lambda, v, h, B_u, B_l, e) = -\varphi(-\varepsilon, \lambda, v, -h, -B_u, -B_l, e), \quad (16)$$

$$\varphi(\varepsilon, \lambda, v, h, B_u, B_l, e) = \varphi(\varepsilon, \lambda, v, h, B_u, -B_l, -e). \quad (17)$$

According with eqs. (15)–(17) it can be deduced without any further calculation that a significant number of coefficients $\varphi_i, \varphi_{ij}, \varphi_{ijk}$ are zero. For instance, from eqs. (15) and (16) it is deduced that the coefficient φ_i multiplying the terms either in B_l or in e must be zero, and from eqs. (16) and (17) the same conclusion with respect to the coefficients of the terms in λ or in v is obtained. Concerning the second-order terms, from eqs. (16) and (17) it is obtained that the coefficients of the terms $\varepsilon^2, v h, \varepsilon B_u, v e, h^2, h B_u, h e, B_l^2, B_u e$, and e^2 must be zero, etc. Therefore, the only first-order coefficients which are non-zero are those corresponding to the terms in h and in B_u , and the second-order coefficients to be taken into account are those in $\varepsilon \lambda, \varepsilon v, \lambda h, \lambda B_u, v h, v B_u$ and $B_l e$. Once the above mentioned non-zero terms are taken into account the only third-order terms that can be of the same order as any of the above mentioned terms are those in $\varepsilon^3, \varepsilon B_l^2$ and εe^2 . Thus the expansion for φ can be simplified to yield

$$\begin{aligned} \varphi = \varphi_4 h + \varphi_5 B_u + 2\varphi_{12} \varepsilon \lambda + 2\varphi_{13} \varepsilon v + 2\varphi_{24} \lambda h \\ + 2\varphi_{25} \lambda B_u + 2\varphi_{34} v h + 2\varphi_{35} v B_u + 2\varphi_{67} B_l e \\ + \varphi_{111} \varepsilon^3 + 3\varphi_{166} \varepsilon B_l^2 + 3\varphi_{177} \varepsilon e^2 + \dots, \end{aligned} \quad (18)$$

where it has been taken into account that $\varphi_{ij} = \varphi_{ji}$ and $\varphi_{iij} = \varphi_{jii} = \varphi_{iji}$. Setting $\varphi = 0$ the original problem is recovered and the value of ε can be deduced as a function of the remaining parameters λ, v, h, B_u, B_l , and e after

$$\begin{aligned} \varphi_4 h + \varphi_5 B_u + 2\lambda(\varphi_{24} h + \varphi_{25} B_u) + 2v(\varphi_{34} h + \varphi_{35} B_u) \\ + 2\varphi_{67} B_l e + 2\varepsilon(\varphi_{12} \lambda + \varphi_{13} v) + 3\varepsilon(\varphi_{166} B_l^2 + \varphi_{177} e^2) \\ + \varphi_{111} \varepsilon^3 \dots = 0. \end{aligned} \quad (19)$$

Note that the terms $2\lambda(\varphi_{24}h + \varphi_{25}B_u)$ and $2v(\varphi_{34}h + \varphi_{35}B_u)$ are negligible when compared with $\varphi_4h + \varphi_5B_u$; therefore, they can be neglected unless $\varphi_4h + \varphi_5B_u = 0$. In the same way the term $3e(\varphi_{166}B_l^2 + \varphi_{177}e^2)$ can be neglected provided $2\varphi_{67}B_l e \neq 0$. Although some of first and second order coefficients have been calculated previously [5, 9, 12, 13], a deduction of all of them, for completeness, can be found in the appendix. It must be pinpointed that φ_{67} is non-zero if $\cos(\beta) \neq 0$. *Perales* [9] concluded that there was no coupling between B_l and e in the stability limit, but there was a mistake in his reasoning, which is only true if $\cos(\beta) = 0$.

Concerning the relevant third order terms, they have been calculated in the past. *Vega* and *Perales* [5] calculated that $\varphi_{111} = -3/2$ and *Perales* [9] calculated that $3\varphi_{166} = -\pi^2/2$ and $3\varphi_{177} = -3/(2\pi^2)$. Thus, eq. (19) reads

$$2\left(B_u - \frac{h}{\pi}\right) - \frac{3}{\pi} B_l e \cos(\beta) + \lambda\left(B_u - \frac{3}{\pi} h\right) + v\left(\frac{3}{2} B_u + \frac{1}{2\pi} h\right) + e(2\lambda + v) - e\left(\frac{\pi^2}{2} B_l^2 + \frac{3}{2\pi^2} e^2\right) - \frac{3}{2} e^3 = 0 \quad (20)$$

where the underlined terms are in most of cases, as already stated, negligible when compared with some other term in the equation.

In order to get a simple analytical expression for the maximum stable slenderness, let us assume that $2(B_u - h/\pi)$ is not too small (when compared with the higher order terms). In this case the first two underlined terms can be neglected (otherwise the algebra is much more involved) and the maximum value of λ (the stability limit, λ_{crit}), which is reached in the point where $d\lambda/de = 0$, is

$$\lambda_{crit} = \left(\frac{3}{2}\right)^{2/3} \left(B_u - \frac{h}{\pi} - \frac{3}{2\pi} B_l e \cos(\beta)\right)^{2/3} - \frac{1}{2} v + \frac{\pi^2}{4} B_l^2 + \frac{3}{4\pi^2} e^2 \quad (21)$$

or, using the original dimensionless variables, to the order here considered the maximum stable slenderness becomes

$$A_{crit} = \pi \left[1 - \left(\frac{3}{2}\right)^{2/3} \left(B_u - \frac{h}{\pi} - \frac{3}{2\pi} B_l e \cos(\beta)\right)^{2/3} + \frac{1}{2} (V - 1) - \frac{\pi^2}{4} B_l^2 - \frac{3}{4\pi^2} e^2 \right] \quad (22)$$

Obviously, eq. (22) is only of application to liquid bridge configurations close enough to the reference one ($B_u = B_l = h = e = 0, V = 1$), but allows us to deduce more general conclusions concerning the influence of the perturbations under consideration on the stability limit. For instance, within this approximation, there is no coupling between the different effects on the variation of the critical slenderness but between B_l and e and, when these two effects are considered, another important feature pointed out by eq. (22) is that A_{crit} does depend on the angle β between the plane defined by the axes of the disks and the direction of the lateral component of microgravity. The variation with the eccentricity e and the angle β of the parameter $V^* = V - 1 - 2(\Lambda/\pi - 1)$, which can represent

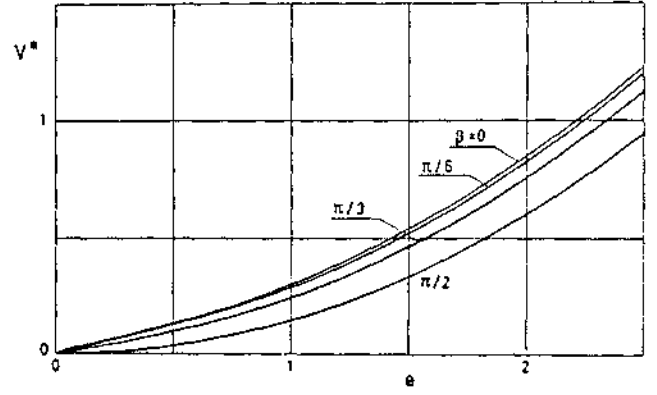


Fig. 2. Variation with the eccentricity of the supporting disks, e , of the reduced minimum volume, $V^* = V - 1 - 2(\Lambda/\pi - 1)$, of liquid bridges between equal disks subjected to a lateral Bond number $B_l = 0.02$

either the minimum stable volume or the maximum stable slenderness, has been plotted in fig. 2 for liquid bridges with $B_u = h = 0$ and $B_l = 0.02$. Note that, for fixed B_l and e , the stability limit can dramatically change depending on the angle β .

Another important characteristic of the stability of liquid bridges that must be remarked is that the combined effect of both lateral Bond number and eccentricity (the term in $B_l e$) can be a stabilizing factor for the liquid column. Observe that, leaving apart the combined effect of axial Bond number and unequal disks, which was already analyzed by *Meseguer* [12], in the case of non-coaxial disks the liquid bridge can be more stable if the acceleration has both axial and lateral components than if only one of them is acting on the liquid bridge.

Finally, let us analyze the importance of the two neglected terms in eq. (20) when eq. (21) was obtained. As already stated these two terms are of importance only when the term powered to $2/3$ in eq. (21) is very small and they give an analytical explanation on the discrepancies previously observed between analytical [12, 14] and numerical [15] results concerning the influence of both axial acceleration and unequal size of the disks on the stability limits of liquid bridges. For the sake of simplicity, let us assume $v = B_l = e = 0$, so that eq. (20) becomes

$$2\left(B_u - \frac{h}{\pi}\right) + \lambda\left(B_u - \frac{3}{\pi} h\right) + 2\lambda e - \frac{3}{2} e^3 = 0 \quad (23)$$

If the underlined term is neglected, the expression $\lambda_{crit} = (3/2)^{2/3} (B_u - h/\pi)^{2/3}$ is obtained (this last expression was the one calculated by *Meseguer* [12]). Such expression has been represented for two different values of h in fig. 3 (dashed lines) and indicate that, up to this order, the maximum stable slenderness will be $A_{crit} = \pi$ at $B_{u,crit} = h/\pi$ no matter what the value of h is, the maximum stable slenderness depending on $|B_u - B_{u,crit}|$. Of course, this behaviour changes when higher order terms are retained. The stability limit which results when the full eq. (23) is used has been represented also in fig. 3 (solid lines). Observe that retaining higher order terms slightly changes the position of the cusp

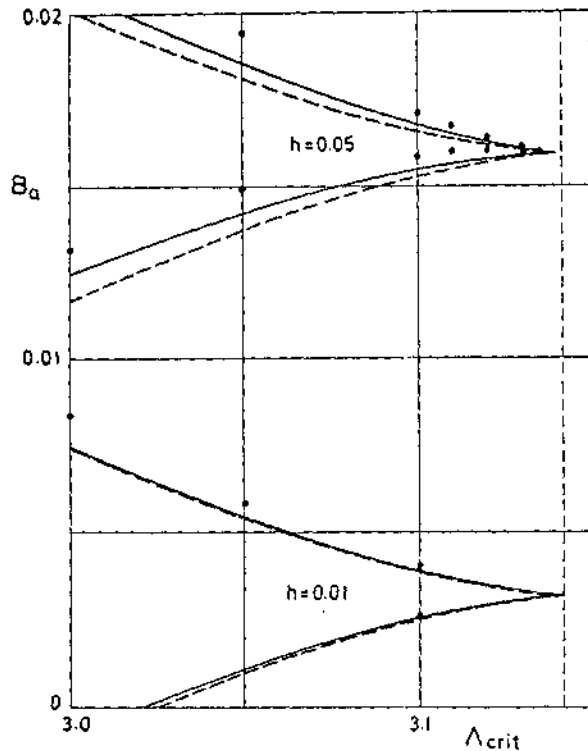


Fig. 3. Variation with the axial Bond number, B_a , of the maximum slenderness, $\Lambda_{crit} = \pi(1 - \lambda_{crit})$, of axisymmetric liquid bridges ($B_t = e = 0$) between unequal disks ($h \neq 0$) having cylindrical volume ($v = 0$). Dashed lines represent the stability limits resulting when the underlined term in eq. (23) is neglected, whereas solid lines represent those obtained when the full eq. (23) is used. The symbols represent numerical results

(although the differences are imperceptible at the used scale) and that the range of stable Bond numbers shifts to larger values. To get an idea of the range of validity of such analytical approximations, some numerical results obtained by using a numerical method already published elsewhere [15] have been also plotted in fig. 3 (black symbols).

3 Experimental Set-up and Experimental Results

The experiments described in the following have been performed in a millimetric liquid bridge facility consisting of a three-axes table in which the liquid bridge is formed. The upper disk can be displaced along the z -axis by means of a micrometric screw whereas the lower disk can be moved along the xy -plane by means of two micrometric screws which displace the lower disk along the x -axis and the y -axis, respectively. Both disks are equal in radius, $R_0 = 0.35$ mm. Fluid injection or removal is made through a hole in the center of the lower disk which is connected to a calibrated syringe. The experimental set-up also includes a CCD camera and a computer with an image processor. To enhance the contour of the liquid bridge interface background uniform illumination was used. The liquid bridge facility and the CCD camera are mounted on a platform which can be oriented at any direction with respect to that of the local gravity acceleration.

The experimental procedure was as follows. First of all, with the disks in coaxial position and the liquid bridge axis vertical, the upper disk is placed close to the lower disk. Then a small amount of working liquid (distilled water) is injected and a small liquid bridge is formed. Once the initial liquid bridge is established, the slenderness is increased by moving upwards the upper disk while additional volume of liquid is injected. The result of this preparation process is a liquid bridge with the desired slenderness and a volume of liquid close to $V = 1$ which is used as a reference to calculate the value of the Bond number. The volume and the Bond number are calculated by fitting theoretical expressions for the liquid bridge equilibrium shapes to the measured shapes by a least square method similar so that described in [14]. The calculated value of the bond number was $B = 0.020 \pm 0.001$.

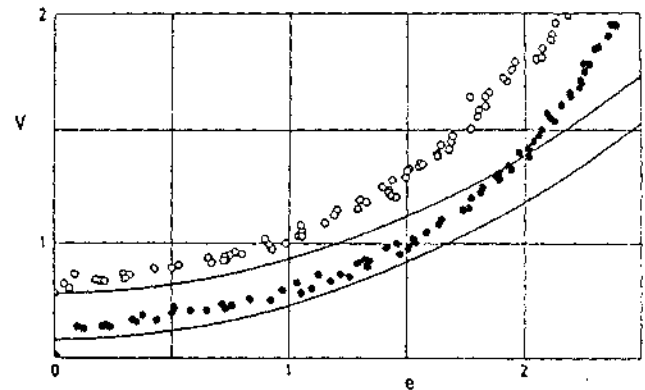


Fig. 4. Minimum volume of the liquid bridge, V , versus eccentricity, e , of liquid bridges between equal disks subjected to a vertical Bond number $B_a = 0.02$. The symbols represent experimental results whereas solid lines correspond to theoretical approximations obtained as indicated in the text. White symbols (upper curve) correspond to liquid bridges with $A = 2.5$ whereas black symbols (lower curve) correspond to liquid bridges with $A = 2.0$

In the case of liquid bridges placed vertically ($B_v \neq 0$, $B_t = 0$), experimental results are shown in fig. 4. In this plot the symbols represent experimental values whereas the curves are theoretical estimations of the stability limits obtained as explained below. As it can be observed there is some scattering in the experimental points, which is due to the way in which the experiments have been done. In effect, although experiments were carefully performed, the handling of the experimental equipment requires the direct manipulation of the facility by the operator. This manipulation, together with the noisy vibrational ambient existing in any Earth laboratory, is the source of uncontrolled perturbations that explain the scattering of the experimental results.

The curves shown in fig. 4 are theoretical estimations according to eq. (22). After this expression, once the slenderness is fixed, the variation with the eccentricity of the minimum stable volume of a liquid bridge between equal disks, when subjected to an axial acceleration ($h = B_t = 0$, $B_v \neq 0$) can be expressed as $V = V_0 + 3e^2/(2\pi^2)$, where V_0 stands for the minimum volume stability limit

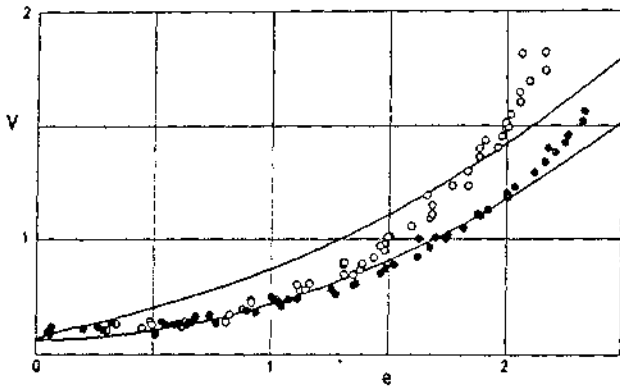


Fig. 5. Minimum volume of the liquid bridge, V , versus eccentricity, e , of liquid bridges between equal disks with slenderness $A = 2.0$ subjected to a lateral Bond number $B_l = 0.02$. The symbols represent experimental results. White (black) symbols correspond to the value $\beta = 0$ ($\beta = \pi/2$) of the angle between the direction in which lateral gravity acts and the plane defined by the axes of the disks whereas solid lines correspond to theoretical approximations obtained as indicated in the text

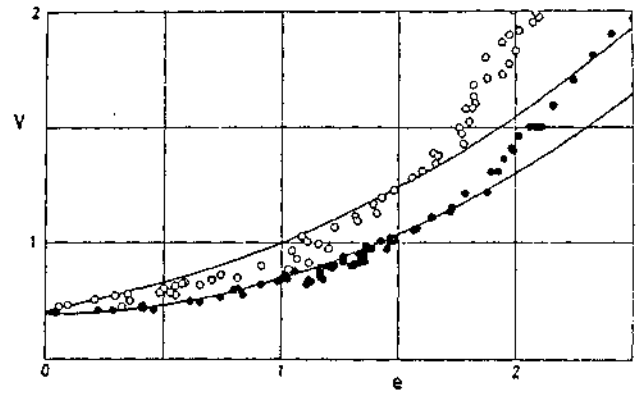


Fig. 6. Minimum volume of the liquid bridge, V , versus eccentricity, e , of liquid bridges between equal disks with slenderness $A = 2.5$ subjected to a lateral Bond number $B_l = 0.02$. The symbols represent experimental results. White (black) symbols correspond to the value $\beta = 0$ ($\beta = \pi/2$) of the angle between the direction in which lateral gravity acts and the plane defined by the axes of the disks whereas solid lines correspond to theoretical approximations obtained as indicated in the text

corresponding to $B_a = 0.02$ and $e = 0$. Obviously, since eq. (22) is only valid close to the reference configuration ($A \sim \pi$, $V \sim 1$, $h \sim 0$, $B_a \sim 0$, $B_l \sim 0$, $e \sim 0$), we cannot expect that the values of V_0 resulting from this expression, $V_0 = 1 + 2(A/\pi - 1) + 2(3/2)^{4/3} B_a^{2/3}$, be a good approximation of the exact values. This is why in fig. 4 the exact theoretical values of V_0 (the minimum volume stability limits corresponding to $h = B_l = e = 0$, $B_a = 0.02$) as reported in [2, 15] have been used instead of those given by eq. (22); these values are $V_0 = 0.580$ at $A = 2.0$ and $V_0 = 0.785$ at $A = 2.5$.

Two main characteristics can be pointed out after the results shown in fig. 4. The first is that the experimental points seem to give higher values of the minimum volume stability limits, even when $e \sim 0$. This can be explained by taking into account, as already remarked, the different sources of perturbations existing in an Earth laboratory, that can cause the breaking of the very small liquid bridges used in experiments when the configuration is close to the stability limit (note that a given perturbation will be more and more important as the size of the liquid bridge decreases). The second aspect to be remarked is that the agreement between theoretical predictions and experimental results is good enough for small values of the eccentricity. Obviously this agreement fails when the eccentricity is large, out of the range of validity of eq. (22).

To experimentally check the influence of the angle β on the stability limits a second set of experiments was performed. In this case the platform which supports the liquid bridge facility and the CCD camera was rotated $\pi/2$, so that the liquid bridge was placed horizontally ($B_a = 0$, $B_l = 0.02$). Experimental results corresponding to $\beta = 0$ and $\beta = \pi/2$, as well as theoretical predictions as given by eq. (22), are shown in fig. 5 for liquid bridges with $A = 2.0$ and in fig. 6 for liquid bridges with $A = 2.5$. In this case the above comment with respect to the value of V_0 still holds; instead of the values of V_0 given by eq. (22) the exact numerical values corresponding to $h = B_a = B_l = e = 0$

(this is, $V_0 = 0.566$ at $A = 2.0$ and $V_0 = 0.693$ at $A = 2.5$) have been used [2, 15]. Observe that experimental results show a behaviour similar to that predicted by eq. (22): liquid bridges are more unstable when lateral gravity acts in a direction parallel to the plane defined by the axes of the disks ($\beta = 0$) than when lateral gravity is normal to this plane ($\beta = \pi/2$). Another aspect to be pointed out is that the agreement between experimental and analytical results increases as the slenderness increases, as one could expect.

4 Conclusions

A theoretical expression for the stability limit of long liquid bridges with an almost cylindrical shape when subjected to a wide variety of perturbations, either axisymmetric or non-axisymmetric, has been obtained. In addition, the dependence of the stability limit on the eccentricity of the supporting disks has been experimentally studied by using millimetric liquid bridges.

It has been demonstrated both theoretically and experimentally that there is a coupling between the two non-axisymmetric effects under consideration (lateral Bond number, B_l , and eccentricity of the supporting disks, e), the magnitude of this coupling depending on the value of the angle β between the direction defined by B_l and the plane formed by the axes of the disks. It must be pointed out that this new term, $B_l e \cos(\beta)$, has an influence on the stability of the liquid column similar to the influence due to axial perturbations like axial Bond number, B_a , or different sizes of the disks, h . This result, somehow surprising, shows that it is possible to stabilize axisymmetric perturbations, like B_a or h , by using combined non-axisymmetric effects like B_l and e .

Appendix

The calculation of the coefficients φ_i , φ_{ij} , φ_{ijk} appearing in eq. (19) requires to solve the problem defined by eq. (11) plus conditions (7)–(10), once the asymptotic expansions

for g , q and φ are introduced in the problem formulation. In order to get more compact expressions for the different problems to be solved, let us include the term $\varepsilon \sin(x)$, which corresponds to the solution of the linear problem, in the series expansion for g , so that the term $\delta_1 g_1$ will be $\delta_1 g_1 = \varepsilon(\tilde{g}_1 + \sin(x))$. With this choice, eq. (11) reads $M^*(1+g) + 1 + q + (1+g)\delta_6 \cos(\theta - \beta) - \delta_5(1 - \delta_2)x + \varphi \sin(x) = 0$, where the small parameters δ_i are as defined in the text. Boundary conditions remain the same, except the condition of volume preservation which, according to the new definition of g_1 , becomes

$$\int_{-\pi}^{\pi} dx \int_0^{2\pi} (2g + g^2) d\theta = 4\pi^2 \delta_3$$

Substitution of the asymptotic expansions for g , q , and φ in the problem formulation gives the following sets of first and second order problems:

First order problems

$$g_{i,v} + g_{i,w} + g_i + \Delta_{i6} \cos(\theta - \beta) - \Delta_{i5} x + q_i + \varphi_i \sin(x) = 0$$

$$g_i(\pm\pi, \theta) = \pm \Delta_{i4} \pm \Delta_{i7} \cos(\theta)$$

$$g_i(x, \theta) = g_i(x, \theta + 2\pi)$$

$$\int_{-\pi}^{\pi} dx \int_0^{2\pi} g_i d\theta = 2\pi^2 \Delta_{i3}$$

where Δ_{ij} stands for the Kronecker delta function ($\Delta_{ij} = 1$ if $i = j$ and $\Delta_{ij} = 0$ if $i \neq j$).

Second order problems

$$g_{i,vv} + g_{i,ww} + g_{ij} + \mathcal{R}_{ij} + q_{ij} + \varphi_{ij} \sin(x) = 0$$

where

$$\begin{aligned} \mathcal{R}_{ij} = & -g_i g_j + \frac{1}{2} g_{i,v} g_{j,v} - \frac{1}{2} g_{i,w} g_{j,w} - g_i g_{j,w} - g_{i,w} g_j \\ & + \frac{1}{1 + \Delta_{ij}} [(1 + \Delta_{i2}) \Delta_{i2} g_{i,v} + (1 + \Delta_{j2}) \Delta_{j2} g_{j,v}] \\ & + \frac{1}{2(1 + \Delta_{ij})} [(1 + \Delta_{i6}) \Delta_{i6} g_i + (1 + \Delta_{j6}) \Delta_{j6} g_j] \cos(\theta - \beta) \\ & + \frac{1}{2} (\Delta_{i5} \Delta_{j2} + \Delta_{i2} \Delta_{j5}) x \end{aligned}$$

$$g_{ij}(\pm\pi, \theta) = -\frac{1}{2} \Delta_{i7} \Delta_{j7} \sin^2(\theta)$$

$$g_{ij}(x, \theta) = g_{ij}(x, \theta + 2\pi)$$

$$\int_{-\pi}^{\pi} dx \int_0^{2\pi} (2g_{ij} + g_i g_j) d\theta = 0$$

Observe that there are $n = 7$ problems of first order and that, because $g_{ij} = g_{ji}$, the number of different problems of second order will be only $n(n+1)/2 = 28$ instead of $n^2 = 49$. Before pursuing further it must be pointed out that since we are interested only in the coefficients φ_i , φ_{ij} , φ_{ijk} , most of the above second order problems have not to be completely solved (obviously all first order problems must be solved because their solutions appear as forcing terms in

the second order problems; and the same happens with some of the second order problems, namely those of order ε^2 , B_i^2 , e^2 , εB_i and εe , because their solutions appear as part of the forcing terms in the relevant third order problems). In effect, let \tilde{g} stand for any of the functions g_i , g_{ij} or g_{ijk} ; it can be easily demonstrated that

$$\begin{aligned} \int_{-\pi}^{\pi} \sin(x) \left[\int_0^{2\pi} (\tilde{g}_{xx} + \tilde{g}_{\theta\theta} + \tilde{g}) d\theta \right] dx \\ = \int_0^{2\pi} [\tilde{g}(\pi, \theta) - \tilde{g}(-\pi, \theta)] d\theta \end{aligned} \quad (A1)$$

Therefore, since all differential equations, no matter what the order is, can be written as $\tilde{g}_{xx} + \tilde{g}_{\theta\theta} + \tilde{g} + \mathcal{R}(x, \theta) + q + \tilde{\varphi} \sin x = 0$, the application of eq. (A1) yields

$$\begin{aligned} \tilde{\varphi} = & -\frac{1}{2\pi^2} \left\{ \int_0^{2\pi} [\tilde{g}(\pi, \theta) - \tilde{g}(-\pi, \theta)] d\theta \right. \\ & \left. - \int_{-\pi}^{\pi} \sin(x) \left[\int_0^{2\pi} \mathcal{R}(x, \theta) d\theta \right] dx \right\}. \end{aligned} \quad (A2)$$

Note that for all second order problems $g_{ij}(\pi, \theta) = g_{ij}(-\pi, \theta)$, so that, in this case eq. (A2) becomes

$$\varphi_{ij} = -\frac{1}{2\pi^2} \int_{-\pi}^{\pi} \sin(x) \left[\int_0^{2\pi} \mathcal{R}_{ij}(x, \theta) d\theta \right] dx. \quad (A3)$$

The solution of the first order problems are

$$\begin{aligned} \hat{g}_1 = 0, & \quad \varphi_1 = 0, \\ \hat{g}_2 = 0, & \quad \varphi_2 = 0, \\ \hat{g}_3 = \frac{1}{2} (1 + \cos(x)), & \quad \varphi_3 = 0, \\ \hat{g}_4 = -\frac{x}{\pi} \cos(x), & \quad \varphi_4 = -\frac{2}{\pi}, \\ \hat{g}_5 = x(1 + \cos(x)), & \quad \varphi_5 = 2, \\ \hat{g}_6 = \frac{1}{2} (\pi^2 - x^2) \cos(\theta - \beta), & \quad \varphi_6 = 0, \\ \hat{g}_7 = \frac{x}{\pi} \cos(\theta), & \quad \varphi_7 = 0, \end{aligned}$$

whereas for the second order problems the application of eq. (A3) gives

$$\begin{aligned} \varphi_{12} = 1, \\ \varphi_{13} = \frac{1}{2}, \\ \varphi_{24} = -\frac{3}{2\pi}, \\ \varphi_{25} = \frac{1}{2}, \\ \varphi_{34} = \frac{1}{4\pi}, \end{aligned}$$

$$\varphi_{35} = \frac{3}{4},$$

$$\varphi_{67} = -\frac{3}{2\pi} \cos(\beta),$$

the remaining coefficients being $\varphi_{ij} = 0$, where most of these zero values were already anticipated in the text after analyzing the symmetries involved in the problem formulation.

Acknowledgments

This work has been supported by the Spanish Comisión Interministerial de Ciencia y Tecnología (CICYT) and is part of a more general endeavour for the study of fluid physics and materials processing under microgravity (Project No. ESP92-0001-CP).

References

- 1 *Myshkis, A. D., Babitskii, V. G., Kopachevskii, N. D., Slobozhanin, L. A., Tyuptsov, A. D.*: Low-gravity Fluid Mechanics. Springer-Verlag, Berlin (1987)
- 2 *Slobozhanin, L. A., Perales, J. M.*: Stability of Liquid Bridges Between Equal Disks in an Axial Gravity Field. *Phys. Fluids A*, vol. 5, p. 1305 (1993)
- 3 *Sanz-Andres, A.*: Static and Dynamic Response of Liquid Bridges; in *Microgravity Fluid Mechanics*, H. J. Rath (ed.), Springer-Verlag, Berlin, p. 3 (1992)
- 4 *Carruthers, J. P., Gibson, E. G., Klett, M. G., Facemire, B. R.*: Studies of Rotating Liquid Floating Zones on Skylab 4. *Prog. Astronaut. Aeronaut.*, vol. 52, p. 207 (1977)
- 5 *Vega, J. M., Perales, J. M.*: Almost Cylindrical Isorotating Liquid Bridges for Small Bond Numbers; in ESA SP-191, p. 247, ESA, Paris (1983)
- 6 *Perales, J. M., Sanz, A., Rivas, D.*: Eccentric Rotation of a Liquid Bridge. *Appl. Microgravity Technol.*, vol. 2, p. 193 (1990)
- 7 *Sanz, A., Perales, J. M., Rivas, D.*: Rotational Instability of a Long Liquid Column, in Final Reports of Sounding Rocket Experiments; in *Fluid Science and Materials Sciences ESA SP-1132 (Vol. 2)*, p. 8, ESA, Paris (1992)
- 8 *Coriell, S. R., Hardy, S. C., Cordes, M. R.*: Stability of Liquid Zones. *J. Colloid Interface Sci.*, vol. 60, p. 126 (1977)
- 9 *Perales, J. M.*: Non-axisymmetric Effects on Long Liquid Bridges. *Acta Astronautica*, vol. 15, p. 561 (1987)
- 10 *Chow, S. N., Hale, J. K.*: *Methods of Bifurcation Theory*. Springer-Verlag, Berlin (1982)
- 11 *Lang, S.*: *Real Analysis*. Addison-Wesley, New York (1969)
- 12 *Meseguer, J.*: Stability of Slender, Axisymmetric Liquid Bridges Between Unequal Disks. *J. Cryst. Growth*, vol. 67, p. 141 (1984)
- 13 *Rivas, D., Meseguer, J.*: One-dimensional Self-similar Solution of the Dynamics of Axisymmetric Slender Liquid Bridges. *J. Fluid Mech.*, vol. 138, p. 417 (1984)
- 14 *Meseguer, J., Mayo, L. A., Llorente, J. C., Fernández, A.*: Experiments with Liquid Bridges in Simulated Microgravity. *J. Cryst. Growth*, vol. 73, p. 609 (1985)
- 15 *Perales, J. M., Meseguer, J., Martínez, I.*: Minimum Volume Stability Limits for Axisymmetric Liquid Bridges Subject to Steady Axial Acceleration. *J. Cryst. Growth*, vol. 110, p. 885 (1991)